POPK-1/Sad-1 kinase is required for the proper translocation of maternal mRNAs and putative germ plasm at the posterior pole of the ascidian embryo

Yoriko Nakamura[1,2,*], Kazuhiro W. Makabe[3] and Hiroki Nishida[1]

[1]Department of Biological Sciences, Graduate School of Science, Osaka University, Machikaneyama-cho, Toyonaka, Osaka 560-0043, Japan
[2]Department of Biological Sciences, Tokyo Institute of Technology, Nagatsuda, Midori-ku, Yokohama 226-8501, Japan
[3]Faculty of Integrated Arts and Sciences, Tokushima University, 1-1 Minami-Josanjima, Tokushima 770-8502, Japan
*Author for correspondence (e-mail: yorinaka@bio.sci.osaka-u.ac.jp)

Accepted 19 August 2005

Development 132, 4731-4742
Published by The Company of Biologists 2005
doi:10.1242/dev.02049

Summary

Maternal mRNAs localized to specific regions in eggs play important roles in the establishment of embryonic axes and germ layers in various species. *Type I postplasmic/PEM* mRNAs, which are localized to the posterior-vegetal cortex (PVC) of fertilized ascidian eggs, such as the muscle determinant *macho-1* mRNA, play key roles in embryonic development. In the present study, we analyzed the function of the *postplasmic/PEM* RNA *Hr-POPK-1*, which encodes a kinase of *Halocynthia roretzi*. When the function of *POPK-1* was suppressed by morpholino antisense oligonucleotides, the resulting malformed larvae did not form muscle or mesenchyme, as in *macho-1*-deficient embryos. Epistatic analysis indicated that POPK-1 acts upstream of macho-1. When *POPK-1* was knocked down, localization of every *Type I postplasmic/PEM* mRNA examined, including *macho-1*, was perturbed, showing diffuse early distribution and eventual concentration into a smaller area. This is the probable reason for the macho-1 dysfunction. The *postplasmic/PEM* mRNAs such as *macho-1* and *Hr-PEM1* are co-localized with the cortical endoplasmic reticulum (cER) and move with it after fertilization. Eventually they become highly concentrated into a subcellular structure, the centrosome-attracting body (CAB), at the posterior pole of the cleaving embryos. The suppression of *POPK-1* function reduced the size of the domain of concentrated cER at the posterior pole, indicating that POPK-1 is involved in the movement of *postplasmic/PEM* RNAs via relocalization of cER. The CAB also shrank. These results suggest that Hr-POPK-1 plays roles in concentration and positioning of the cER, as well as in the concentration of CAB materials, such as putative germ plasm, in the posterior blastomeres.

Key words: Ascidian embryo, *Halocynthia roretzi*, RNA localization, *postplasmic/PEM* RNA, Cortical endoplasmic reticulum, Germ plasm, POPK-1 kinase, Sad-1 kinase

Introduction

mRNA localization occurs in a diversity of organisms, ranging from yeasts to plants and animals. It plays important roles in embryonic axis formation, cell polarity, asymmetric cell divisions and cell differentiation in eggs, embryos and somatic cells such as fibroblasts and neurons (Kloc et al., 2002). In many cases, mRNA localization is coupled with translational control. In flies and vertebrates, the restriction of some localized mRNAs to a particular region is important for their translation. This enables proteins to be synthesized at the right time in the right place (Lipshitz and Smibert, 2000; Johnstone and Lasko, 2001; Palacios and Johnston, 2001; Yoshida et al., 2004). In *Xenopus* and *Drosophila*, maternal factors segregate in distinct regions of the egg and blastomeres, and in many cases these factors are maternal mRNAs produced during oogenesis. For example, *bicoid* and *oskar* mRNAs are localized to the anterior and posterior poles in *Drosophila* eggs and determine the anterior-posterior axis and germ cell formation (Riechmann and Ephrussi, 2001). In *Xenopus* eggs, several maternal transcripts are specifically localized in the animal or vegetal cortex of eggs. In particular, *VegT* mRNA localization in the vegetal cortex is crucial for endomesoderm formation, and *Xcat2* for germ cell differentiation (King et al., 1999).

In ascidians, several maternal mRNAs are located in the posterior-vegetal cortex (PVC) of fertilized eggs just before cleavage. Micromanipulation experiments in which PVC is deleted and transplanted have shown that it is possible to remove and transplant the potential for formation of the posterior tissues, including muscle, and for unequal cleavages that are characteristic of the posterior pole. By contrast, the removal and transplantation of the egg cytoplasm of other regions have no effect (Nishida, 1994). When PVC is removed from eggs, mirror-image duplication of the anterior half occurs in the cell fates and cleavage pattern. Muscle and mesenchyme precursor blastomeres are converted to nerve cord and notochord, respectively, so that central endoderm blastomeres are encircled by these blastomeres (Nishida, 1994; Kobayashi et al., 2003). The transplantation of the PVC to the anterior

region of the PVC-deficient eggs reversed the anteroposterior axis. Therefore, localized factors in the PVC play critical roles in the determination of the anteroposterior axis, which is involved in autonomous specification of muscle fate, generation of differences in responsiveness to inductive signals in mesenchyme and notochord precursor blastomeres, and control of cleavage pattern (reviewed by Nishida, 1997; Nishida, 2002; Nishida, 2005).

In eggs of *Halocynthia roretzi*, nine maternal mRNAs localized to the PVC have been identified so far, including *macho-1*, the muscle and posterior determinant. They are called *Type I postplasmic/PEM* mRNAs (Sasakura et al., 1998a; Sasakura et al., 1998b; Nishida and Sawada, 2001; Makabe et al., 2001; Nakamura et al., 2003) (reviewed by Sardet et al., 2005). They show identical localization during cytoplasmic and cortical reorganization, so-called ooplasmic segregation in ascidians, and are concentrated in the centrosome-attracting body (CAB) during early cleavages. The CAB was first found as a small subcellular structure that operates cleavage planes during successive unequal cleavages at the posterior pole (Hibino et al., 1998; Nishikata et al., 1999) (reviewed by Nishida et al., 1999). Every *Type I postplasmic/PEM* mRNA is localized to the CAB at the 8-cell stage (Sasakura et al., 2000; Nakamura et al., 2003; Sardet et al., 2003). Thus, the CAB serves as the core structure of a multifunctional complex that operates cleavage planes and anchors *Type I postplasmic/PEM* RNAs. Having both functions together, the CAB ensures that *Type I postplasmic/PEM* RNAs are infallibly partitioned into one of the daughter cells after cell divisions.

Another conspicuous characteristic of the CAB is that it is enriched in putative germ plasm. An electron microscopic study revealed that the CAB contains an electron-dense matrix (EDM) that resembles germ plasm in other animals (Iseto and Nishida, 1999). The CAB is eventually segregated into the putative germline cells, the posteriormost and smallest blastomeres (B7.6 cells) of the 64-cell embryos (Fujimura and Takamura, 2000; Takamura et al., 2002) (reviewed by Nishida, 2005). Various observations support the view that B7.6 cells are primordial germ cells in ascidians, and that the CAB, enriched in *postplasmic/PEM* RNAs, also contains putative germ plasm. As *Halocynthia* eggs are translucent, the CAB can be seen in extracted and cleared embryos. In such extracted embryos, only the EDM seems to persist in the CAB as a highly refractive structure under an optical microscope (Iseto and Nishida, 1999).

Maternal mRNAs accumulated in the CAB are categorized into two groups. *Type I postplasmic/PEM* mRNAs are already localized to the PVC before cleavage starts. Some of them, such as *macho-1* and *Hr-PEM1*, have been shown to associate with the cortical endoplasmic reticulum (cER) tethered to the plasma membrane of the egg, and they are concentrated into the CAB together with the cER by the 8-cell stage (Sardet et al., 2003; Sardet et al., 2005). Consequently, the CAB is enriched in cER and *Type I postplasmic/PEM* mRNAs. By contrast, *Type II postplasmic/PEM* mRNAs are distributed evenly throughout the egg cytoplasm, and then gradually concentrate into the CAB during cleavages. *Cs-PEM* is the *Type I postplasmic/PEM* mRNA first found in ascidians (Yoshida et al., 1996). A complete list of *Type I* and *Type II postplasmic/PEM* mRNAs in three ascidian species are available in Makabe et al. (Makabe et al., 2001) and Sardet et al. (Sardet et al., 2005). Experiments with cytoskeletal inhibitors showed that distinct mechanisms are involved in the localization of *Type I* and *Type II* mRNAs to the CAB (Sasakura et al., 2000), although the localization mechanism still remains largely unknown. The results of the removal and transplantation of the PVC of eggs indicate that *Type I postplasmic/PEM* mRNAs are more important than *Type II*. The crucial functions in early development of *macho-1* and three other *Type I postplasmic/PEM* mRNAs (*Hr-Wnt-5*, *Hr-GLUT* and *Hr-PEN2*) in *Halocynthia* have been investigated (Nishida and Sawada, 2001; Kobayashi et al., 2003; Nakamura et al., 2005).

Halocynthia roretzi-posterior protein kinase-1 (*Hr-POPK-1*) is a *Type I postplasmic/PEM* mRNA and encodes a serine/threonine kinase (Sasakura et al., 1998b). The expression is strictly maternal during embryogenesis. Hr-POPK-1 protein shares high similarity to Sad-1 of *Caenorhabditis elegans* and SAD-A of mouse throughout its entire length (Crump et al., 2001; Kishi et al., 2005) (Fig. 1). Humans and *Drosophila* also have several proteins very similar to POPK-1/Sad-1/SAD-A, although their functions in these animals are not known. Therefore, POPK-1 is a member of a group of proteins widely conserved among metazoans. Three domains are conserved between these proteins: a kinase domain, a domain next to the kinase domain and a domain in the C-terminal half. The latter two domains show no similarity to domains with known functions. Crump et al. (Crump et al., 2001) reported that the kinase domain of Sad-1 has extensive similarity to that of Par-1, which plays a central role in specification of the anterior-posterior polarity in *C. elegans*

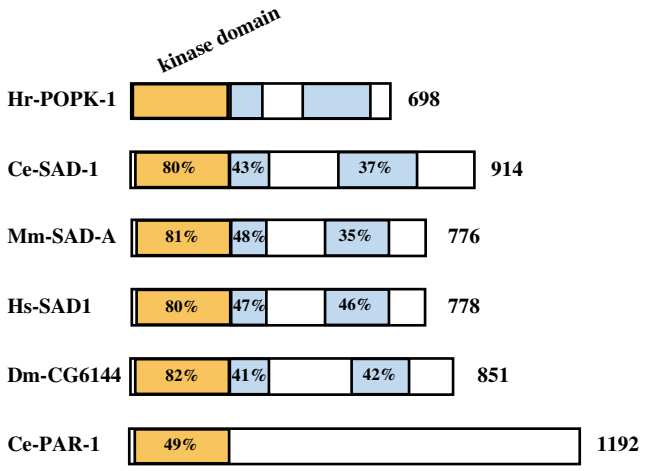

Fig. 1. Comparisons of Hr-POPK-1 with homologs in other animals. Hr-POPK-1 shows high similarity to Cs-SAD-1 of *C. elegans* (Accession No. AB014885), Mm-SAD-A of mouse (Accession No. AY533671), Hs-SAD1 of human (Accession No. BC016681) and CG6144 of *Drosophila melanogaster* (Accession No. NM135570). Humans have at least three other homologs in the genome. These proteins share an N-terminal kinase domain (orange). The amino acid identity compared with Hr-POPK-1 is indicated in the diagrams. They had two other conserved domains (blue), whose function is unknown. Hr-POPK-1 and PAR-1 of *C. elegans* show lower similarity in their kinase domains, and PAR-1 has no similarity outside the kinase domain. Numbers on the right side indicate the number of total amino acid residues.

eggs. However, similarity is lower in the Par-1 kinase domain, and Par-1 has no conserved domains other than the kinase domain (Fig. 1). To investigate the functions of *Hr-POPK-1*, we injected eggs with specific antisense morpholino oligonucleotides (MOs). The results indicate that Hr-POPK-1 is required for proper transport of the *Type I postplasmic/PEM* mRNAs during cleavages via regulation of concentration and positioning of the cER, as well as for proper CAB formation.

Materials and methods

Animals and embryos

Adults of the ascidian *Halocynthia roretzi* were collected near the Asamushi Research Center for Marine Biology, Aomori, Japan, and the Otsuchi International Coastal Research Center, Iwate, Japan. Naturally spawned eggs were fertilized with a suspension of non-self sperm and raised in Millipore-filtered seawater containing 50 μg/ml streptomycin sulfate and 50 μg/ml kanamycin sulfate at 9-13°C.

Microinjection of MOs and synthetic mRNA

To suppress the function of *Hr-POPK-1,* we used two MOs (Gene Tools). The sequences of the MOs against *Hr-POPK-1* (Accession No. AB014885) were as follows: *Hr-POPK-1* MO1 (5′-CGGCGC-ATTTGACATTTTAAAGAAA-3′), which covers the starting methionine, and *Hr-POPK-1* MO2 (5′-TGTTCAGTTCAAATGAC-ACAATAAA-3′), which covers the 5′ UTR. As a control MO, we used standard control oligo (5′-CCTCTTACCTCAGTTACAATT-TATA-3′), 5-mismatch control MO (5′-TCTTGAGTTGAAATCA-CAGAATAAA-3′; mismatches underlined), and *PEN1* MO (5′-CGTAAACAGTAGGAACAATTTCATA-3′). *macho-1* MO was the same as used previously (Kobayashi et al., 2003). We injected 500 pg of *Hr-POPK-1* MO1 and 750 pg of *Hr-POPK-1* MO2 and control MOs into the fertilized eggs. *Hr-POPK-1* mRNA was transcribed from pBluescriptHTB containing the *Hr-POPK-1* open reading frame with a mMessage mMachine T3 kit (Ambion) and a Poly (A) Tailing kit (Ambion). *macho-1* mRNA was synthesized as described previously (Kobayashi et al., 2003). MO and synthetic mRNA were dissolved in sterile distilled water and injected into ascidian eggs as described by Miya et al. (Miya et al., 1997).

Immunostaining, histochemical staining and in-situ hybridization

The monoclonal antibody Mu-2 was used for monitoring muscle formation (Nishikata et al., 1987). This antibody recognizes the myosin heavy chain in tail muscle cells of *Halocynthia* larvae (Makabe and Sato, 1989). The monoclonal antibody Mch-3 was used to detect mesenchyme formation (Kim and Nishida, 1998). The specimens were fixed after the hatching stage for 10 minutes in methanol at –20°C. Formation of notochord cells was monitored by staining with the Not-1 monoclonal antibody (Nishikata and Satoh, 1990; Nakatani and Nishida, 1994). Specimens were fixed at the tailbud stage. Indirect immunofluorescence was carried out by standard methods using a TSA fluorescein system (Perkin-Elmer Life Sciences). Then specimens were mounted in 80% glycerol and examined under a fluorescence microscope. In some cases embryos were allowed to develop up to the 110-cell stage and transferred to seawater containing 2.5 μg/ml cytochalasin B (Sigma) to permanently arrest further cleavage.

To detect muscle formation, we also used histochemical detection of acetylcholinesterase (AChE) as described by Karnovsky and Roots (Karnovsky and Roots, 1964). Specimens at the tailbud stage were fixed in 5% formalin in seawater for 10 minutes at room temperature. The reaction was performed at 4°C for 16 hours to reveal the presence of the AChE (brown products). Formation of endoderm was monitored by histochemical detection of alkaline phosphatase (ALP) activity by using the methods described by Meedel and Whittaker (Meedel and Whittaker, 1989). Embryos were fixed for 1 minute in 70% ethanol at –20°C. Specimens were treated with ALP detection buffer for monitoring purple products.

Whole-mount in-situ hybridization was performed as described by Miya et al. (Miya et al., 1994; Miya et al., 1997). Specimens were hybridized with digoxigenin (DIG)-labeled *macho-1*, *Hr-PEM1* (Nishida and Sawada, 2001), *Hr-POPK-1* (Sasakura et al., 1998b), *Hr-ZF1* (Sasakura et al., 2000), *Hr-Wnt-5* (Sasakura et al., 1998a) and *Hr-PEN1* (Nakamura et al., 2003) antisense RNA probes.

Reverse transcription-polymerase chain reaction

Reverse transcription-polymerase chain reaction (RT-PCR) was carried out with a Cells-to-cDNA II kit (Ambion) according to the manufacturer's protocol. Ten embryos at the 8-cell stage, which were devitellinated with a fine tungsten needle, were lysed in 100 μl Cell Lysis II Buffer and used for cDNA synthesis. PCR was carried out using the following *macho-1* primers: 5′-GAATAATCCACACGCTT-3′ and 5′-GCTTGGTTTCGCCTAA-3′, *Hr-POPK-1* primers; 5′-GTATCGCATACACTGTTG-3′ and 5′-AAATGGAGCAGTTCCT-TG-3′, *Hr-ZF1* primers; 5′-AATTCCTCCCCTGGTTGA-3′ and 5′-TGATTTGGTGGAACACAAC-3′, and *Hr-Notch* primers as a loading control; 5′-TCTACCCTTTTGCTATTCC-3′ and 5′-ATT-TGTCACTTAGAATTAAGA-3′. PCR was performed for 34 cycles for *Hr-POPK-1*and *HrZF-1*, and 35 cycles for *macho-1* and *Hr-Notch*, at 94°C for 1 minute, 50°C (53°C for *Hr-POPK-1*) for 1 minute and 72°C for 1 minute. The PCR products were resolved by 1-2% agarose gel electrophoresis.

Extraction of embryos

To visualize the CAB, embryos were extracted and cleared. Dechorionated 8-cell stage embryos were rinsed twice with Ca^{2+}-, Mg^{2+}-free artificial seawater containing 1 mmol/l EGTA, and transferred to an extraction buffer composed of 50 mmol/l $MgCl_2$, 10 mmol/l KCl, 10 mmol/l EGTA, 2% Triton X-100, 20% glycerol, and 25 mmol/l imidazole (pH 6.9) for 1-2 hours (Nishikata et al., 1999). During extraction, the embryos become transparent. The CABs of the extracted embryos were observed using Nomarski optics.

Isolation of cortices

Isolation of cortices of eggs and of 2-, 4-, and 8-cell-stage embryos and fluorescence (TSA) in-situ hybridization with isolated cortices were carried out as described previously (Sardet et al., 2003). The cER network of isolated cortices was labeled in red with a lipophilic dye, $DiIC_{18}$ (3) (Molecular Probes).

Results

POPK-1 is required for muscle formation

To investigate the function of *POPK-1* in ascidian development, we used specific MOs to inhibit its translation. MOs are effective in specifically preventing the functions of various genes in ascidian embryos (e.g. Satou et al., 2001). We designed two MOs against different non-overlapping sequences of *Hr-POPK-1* (MO1 and MO2) to confirm their specificity. As both of them gave very similar results, the specificity of these MOs were supported, and we present the results without discrimination between the two (most results were obtained with MO2). Most embryos injected with *POPK-1* MO developed normally up to the 110-cell stage, although a few showed a radialized cleavage pattern, as described later. Then gastrulation became aberrant. Eventually, the morphology of larvae was severely affected. The tail was not obvious, and no sensory pigment cells were present (Fig. 2A′). The degree of malformation was dose dependent. The morphology of larvae injected with standard control MO and

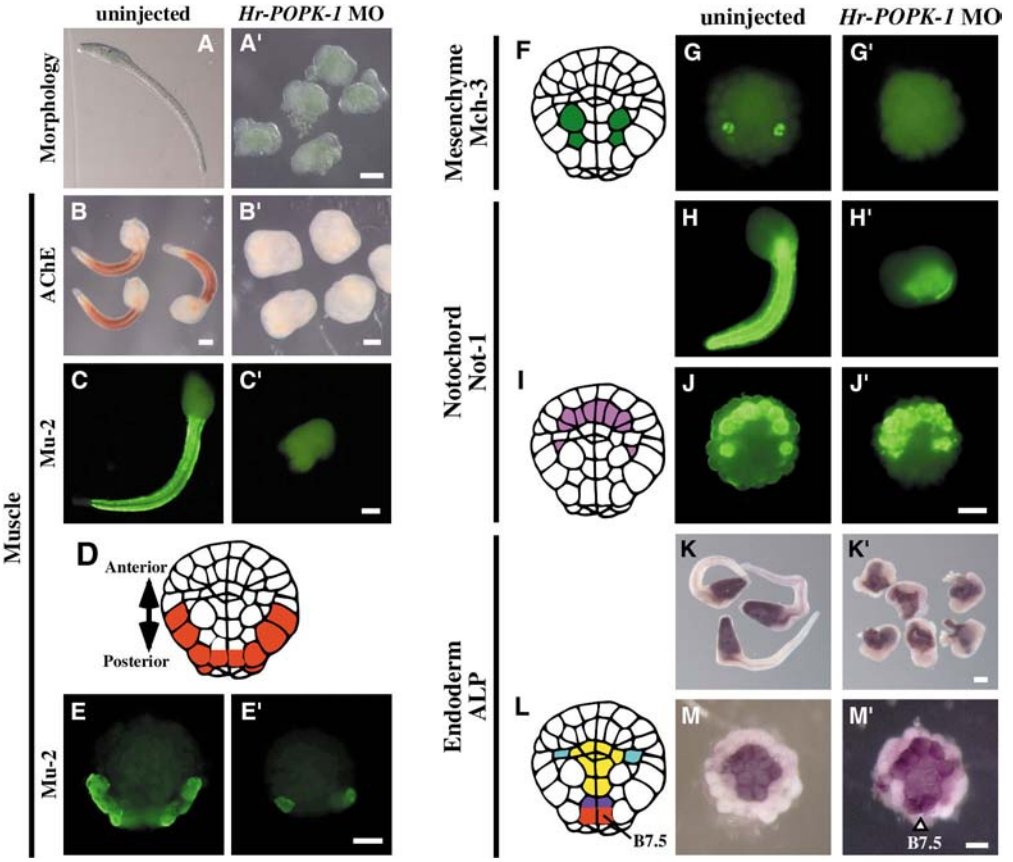

Fig. 2. Tissue formation in embryos injected with *POPK-1* MO. (A-C,E,G-M) Uninjected controls. (A′-C′,E′,G′-M′) *POPK-1* MO was injected into fertilized eggs after the completion of ooplasmic segregation. (D,F,I,L) Diagram of the vegetal hemisphere at the 110-cell stage, showing presumptive muscle, mesenchyme, notochord and endoderm blastomeres, respectively. Anterior is up. In (L), endoderm precursors are yellow, trunk lateral cell precursors are blue. B7.5 blastomeres give rise to muscle (red) and trunk ventral cells (purple). (A,A′) Morphology. (B,B′) Expression of muscle-specific acetylcholinesterase (AChE) in tailbud embryos. (C,C′) Expression of myosin protein (Mu-2 antigen) in larvae. (E,E′) Expression of myosin in embryos whose cleavages were arrested at the 110-cell stage. (G,G′) Mesenchyme-specific Mch-3 antigen in cleavage-arrested embryos. (H,H′) Notochord-specific Not-1 antigen. (J,J′) Not-1 antigen in cleavage-arrested embryos. (K,K′) Expression of alkaline phosphatase (ALP). (M,M′) ALP in cleavage-arrested embryos. Ectopic ALP activity is observed in the posteriormost (B7.5) cells (arrowhead) in (M′). Scale bars: 100 μm.

5-mismatch control MO was normal. However, the aberrant development of *POPK-1* MO-injected embryos was not rescued by co-injection of *POPK-1* mRNA lacking morpholino target sequences.

We examined muscle formation in embryos injected with MO by monitoring the expression of acetylcholinesterase (AChE), a muscle-specific enzyme. Uninjected and control MO-injected larvae looked normal, and AChE was expressed in tail muscle cells (Fig. 2B). In embryos injected with *POPK-1* MO, however, AChE expression was severely reduced or abolished (Fig. 2B′). Suppression of muscle formation was confirmed by immunostaining with the myosin antibody Mu-2 (Fig. 2C,C′). Absence of muscle cells was further confirmed in embryos in which cleavage was arrested at the 110-cell stage. Even when cleavage is permanently arrested at the 110-cell stage by treatment with cytochalasin B, ascidian embryos continue some differentiation and eventually express tissue differentiation features (Whittaker, 1973). In cleavage-arrested embryos uninjected or injected with control MO, ten muscle precursor blastomeres expressed Mu-2 and AChE, as expected from the fate map (Fig. 2D,E). By contrast, in embryos injected with *POPK-1* MO, the number of positive blastomeres was greatly reduced (Fig. 2E′, Table 1).

The phenotype of *POPK-1*-deficient embryos resembles that of *macho-1*-deficient embryos

In *macho-1*-deficient embryos, primary muscle cells are lost, and the formation of other tissues is also affected (Nishida and Sawada, 2001; Kobayashi et al., 2003). To investigate the possibility that *POPK-1* might have a similar role to *macho-1*, we analyzed the formation of mesenchyme, notochord and endoderm in embryos with MO. The presence of mesenchyme cells was examined with the monoclonal antibody Mch-3. When cleavage was arrested at the 110-cell stage, four presumptive mesenchyme blastomeres expressed the Mch-3 antigen in control embryos (Fig. 2F,G). By contrast, the mesenchyme marker was rarely expressed in MO-injected embryos (Fig. 2G′, Table 1). Notochord formation was evaluated with Not-1 antibody. Inhibition of *POPK-1* function did not affect the expression of the Not-1 antigen at the tailbud stage (Fig. 2H,H′). In cleavage-arrested embryos, the arrangement and maximum number of Not-1-positive cells coincided well with notochord-lineage cells at the 110-cell stage in controls (Fig. 2I,J). There was no notable difference between control embryos and *POPK-1* MO-injected embryos (Fig. 2J′, Table 1).

Endoderm differentiation was monitored by detecting the expression of alkaline phosphatase (ALP). The suppression of *POPK-1* function did not seem to affect ALP expression at the larval stage (Fig. 2K,K′). This was essentially confirmed in cleavage-arrested embryos. In both control embryos and MO-injected embryos, ALP activity was observed in ten endoderm precursors and two presumptive trunk lateral cells (TLCs) (Fig. 2L,M). However, in 15% of MO-injected embryos, ectopic ALP activity was observed in the posteriormost (B7.5) cells,

Table 1. Effects of inhibition of *POPK-1* function on tissue differentiation

	Embryos with expression of markers / embryos examined (%)								
	Control MO (750 pg)				*Hr-POPK-1* MO2 (750 pg)				
Marker	*n*	Normal	Reduced	Not detected	*n*	Normal	Increased	Reduced	Not detected
Muscle (AChE)	29 (41)	**100 (95)**	0 (5)	0 (0)	25 (11)	0 (0)	0 (0)	28 (45)	**72 (55)**
(Mu-2)	37 (15)	**100 (94)**	0 (6)	0 (0)	63 (21)	16 (0)	0 (0)	36 **(100)**	**48** (0)
Mesenchyme (Mch-3)	23 (24)	**100 (92)**	0 (4)	0 (4)	27 (26)	4 (4)	0 (0)	4 (23)	**92 (73)**
Notochord (Not-1)	11 (10)	**100 (100)**	0 (0)	0 (0)	18 (21)*	**78 (48)**	0 (0)	0 (33)	22 (19)
Endoderm (ALP)	15 (26)	**100 (100)**	0 (0)	0 (0)	25 (26)	**84 (85)**	0 (15)	16 (0)	0 (0)

**Hr-POPK-1* MO1 was injected.
Results of cleavage-arrested embryos are indicated in parentheses.
Highest proportions are indicated in bold.

which are presumptive muscle blastomeres (Fig. 2M′, arrowheads; Table 1, parentheses).

Loss of muscle and mesenchyme, normal formation of notochord, and transformation of B7.5 blastomere into endoderm were common to embryos injected with a low dose of *macho-1* MO (Kobayashi et al., 2003). A high dose of *macho-1* MO injection resulted not only in the loss of muscle and mesenchyme, but also in ectopic notochord formation in the posterior region in place of original mesenchyme blastomeres, so that central endoderm blastomeres were encircled by notochord blastomeres. This anteriorization was also observed in embryos from which the posterior-vegetal cortex (PVC) was removed (Kobayashi et al., 2003). However, ectopic notochord formation was never observed in *POPK-1* MO-injected embryos. These observations suggest that the phenotype of *POPK-1* MO-injected embryos resembles that of embryos in which the function of *macho-1* is partially inhibited. This is supported by the results of the following experiments.

Hr-POPK-1 acts upstream of *macho-1*

Fertilized eggs injected with *Hr-POPK-1* mRNA (100-300 pg) cleaved normally, and the larvae had almost normal morphology, with sensory pigment cells, palps and elongated tails, which were sometimes kinked (Fig. 3A,A′). There was no excess muscle formation in cleavage-arrested embryos, by contrast to those injected with *macho-1* mRNA (normal in 97% of 44 cases, Fig. 3B,B′). The results indicate that POPK-1 is required but not sufficient for muscle formation.

Then we analyzed the epistatic relationship between *POPK-1* and *macho-1* by monitoring muscle formation. When *macho-1* MO (60-120 pg, low dose) was injected into fertilized eggs, the number of muscle cells in larvae was significantly reduced (Nishida and Sawada, 2001) (compare Fig. 3C,D). Co-injection with *POPK-1* mRNA (230 pg) had no rescuing activity, as tail formation was still severely affected, and the number of muscle cells was similar to that in embryos injected only with *macho-1* MO (compare Fig. 3D,E). However, when *POPK-1* MO2 (750 pg) and *macho-1* mRNA (120 pg) were co-injected, excess muscle formed (Fig. 3F, Table 2). These results suggest that the suppression of *Hr-POPK-1* function affects muscle cell formation through *macho-1*, and that POPK-1 acts upstream of macho-1.

POPK-1 is required for proper localization of *macho-1* mRNA during early cleavage stage

As *macho-1* mRNA is a localized muscle determinant and POPK-1 acts upstream of macho-1, we then examined whether the localization of *macho-1* mRNA in the CAB at the 8-cell stage is altered in embryos injected with *POPK-1* MO. In normal embryos, *macho-1* mRNA accumulated in a moustache-shaped CAB in the posterior cortex of posterior-

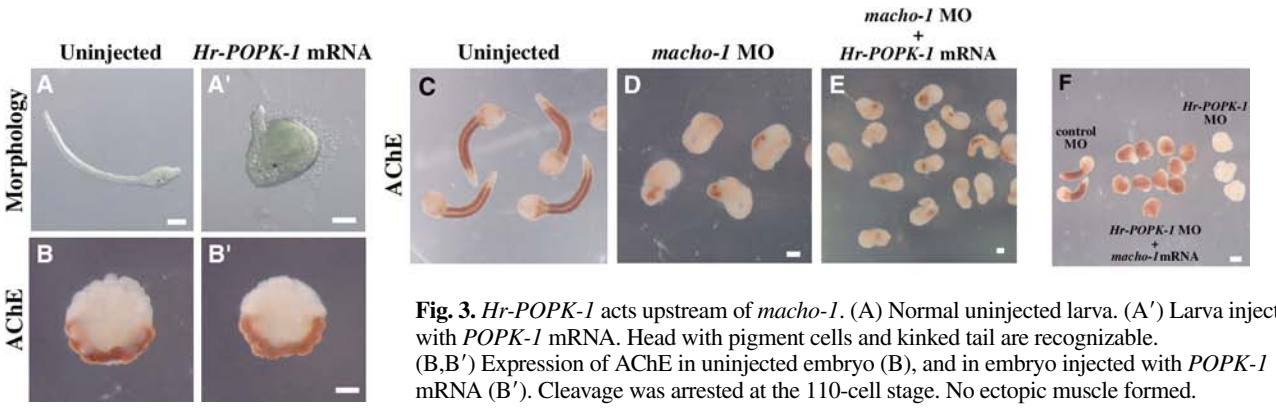

Fig. 3. *Hr-POPK-1* acts upstream of *macho-1*. (A) Normal uninjected larva. (A′) Larva injected with *POPK-1* mRNA. Head with pigment cells and kinked tail are recognizable. (B,B′) Expression of AChE in uninjected embryo (B), and in embryo injected with *POPK-1* mRNA (B′). Cleavage was arrested at the 110-cell stage. No ectopic muscle formed. (C-E) Expression of AChE in uninjected tailbud embryos (C), in embryos injected with *macho-1* MO (D) and in embryos co-injected with *macho-1* MO and *POPK-1* mRNA (E). Loss of muscle cell was not rescued by co-injection of the mRNA. (F) Expression of AChE in embryos injected with control MO (left), in embryos co-injected with *POPK-1* MO and *macho-1* mRNA (center) (excess amounts of muscle cells are formed), and in embryos injected with *POPK-1* MO (right) (no muscle is formed). Scale bars: 100 μm.

Table 2. Effect of co-injection of *POPK-1* MO and *macho-1* mRNA on muscle formation in cleavage-arrested embryos

		AChE expression (%)			
	n	Increased	Normal	Reduced	Not detected
Uninjected embryos	15		**100**	0	0
Control MO (750 pg)	16		**100**	0	0
Hr-POPK-1 MO2 (750 pg)	13		0	8	**92**
Hr-POPK-1 MO2 (750 pg) + *macho-1* mRNA (120 pg)	26	**89**	11	0	0

Highest proportions are indicated in bold.

vegetal B4.1 blastomeres (79% of 29 cases, Fig. 4A, arrowheads). At the early 8-cell stage, embryos injected with *POPK-1* MO, *macho-1* mRNA was more diffuse (all 18 cases, Fig. 4A, arrowheads). By contrast, at the late 8-cell stage, *macho-1* mRNA became concentrated in smaller bilateral globular dots, instead of a normal elongated distribution (all 38 cases, Fig. 4A, arrowheads). In normal embryos the localization was connected on both sides of the midline, as the CAB is connected, but in injected embryos small dots were always visible apart from the midline. It is noteworthy that the small staining was always present but never lost in every case. *Hr-PEN1* is a *Type I postplasmic/PEM* mRNA and has similarity to mammalian *g1*-related protein (Nakamura et al., 2003). To carry out more precise control experiments, we injected MO against *PEN1*, and *macho-1* mRNA was normally localized like a moustache (data not shown). The result further supports that the aberrant localization of *macho-1* mRNA is caused by specific inhibition of the *POPK-1* function.

We then examined *macho-1* localization at the 2-, 4-, 16- and 32-cell stages. In the 2- and 4-cell embryos, localization in the mRNA-rich posterior cortical region seemed to be broader and more diffuse than that in control embryos (Fig. 4B, arrowheads). The diffuse distribution coincides well with that observed at the early 8-cell stage. Because the *POPK-1* MO was injected into fertilized eggs after the completion of ooplasmic segregation, MO did not affect ooplasmic segregation. The effect observed at the 2-cell stage suggests that POPK-1 translation starts as early as the 2-cell stage, and MO interfered with its functions. At the 16- and 32-cell stages, *macho-1* mRNA was localized in smaller dots at the posterior pole (Fig. 4B, arrowheads), as observed in the late 8-cell embryos. Therefore, transition from diffuse to compact distribution occurs at the middle 8-cell stage.

To evaluate the quantity of *macho-1* mRNA, we carried out semi-quantitative RT-PCR using 8-cell embryos. *macho-1* mRNA was amplified from ten embryos with and without MO. As shown in Fig. 4C, the amount of *macho-1* mRNA seems to be slightly reduced in MO-injected embryos relative to uninjected embryos at the late 8-cell stage, but not completely abolished. This coincides with the result of in-situ hybridization. The result was confirmed in three independent experiments using different batches of eggs. We tentatively quantified the intensity of the bands with the software NIH Image. The intensity was reduced to 60% on average.

Hr-POPK-1 is involved in every *Type I postplasmic/PEM* mRNA localization and in proper CAB formation

To test whether the distributions of other *Type I postplasmic/PEM* mRNAs are also affected, embryos were probed for five other *Type I postplasmic/PEM* mRNAs: *Hr-PEM1*, *Hr-POPK-1*, *Hr-ZF1*, *Hr-Wnt-5* and *Hr-PEN1* mRNAs. In embryos injected with control MO, the distributions of all these mRNAs were normal (Fig. 4C, left, arrowheads). In embryos injected with *POPK-1* MO, the distribution of these mRNAs was reduced in size (Fig. 4C, right, arrowheads: *Hr-PEM1*, 83% of 30 cases; *Hr-POPK-1*, 75% of 8 cases; *Hr-ZF1*, 86% of 22 cases; *Hr-Wnt-5*, 100% of 10 cases; and *Hr-PEN1*, 100% of 21 cases). The phenotype was identical to that observed for *macho-1* distribution. These results demonstrate that *POPK-1* MO affects the distribution of every *Type I postplasmic/PEM* mRNA, including *POPK-1* itself. We also carried out semi-quantitative RT-PCR at the late 8-cell stage to evaluate the quantity of *Hr-POPK-1* and *Hr-ZF1* mRNA, and *Hr-Notch* mRNA as loading control. By contrast to *macho-1*, there was no remarkable difference in the amount of *POPK-1* and *Hr-ZF1* mRNA between uninjected embryos and MO-injected embryos (Fig. 4D). The result was confirmed in three independent experiments using different batches of eggs. The intensity of the band was 94%, 110% and 91% on average for *Hr-POPK-1*, *Hr-ZF1* and *Hr-Notch*, respectively, compared to uninjected embryos.

These *postplasmic/PEM* mRNAs are present in the CAB at the 8-cell stage. Therefore, we observed the shape of the CAB in extracted and cleared embryos. In uninjected embryos, control MO- and *PEN-1* MO-injected embryos, the CAB appeared as two bars connected at the midline in the posterior cortex of the posterior blastomeres after extraction at the late 8-cell stage (Fig. 5A, arrowhead). By contrast, in embryos injected with *POPK-1* MO, the CAB appeared as two small dots apart from the midline in the posterior cortex (Fig. 5B, arrowhead; 90% of 31 cases). In spite of this shrinkage, the small CAB was always present and never lost. This observation indicates that not only mRNA distribution, but also the CAB itself, shrank.

The CAB in extracted embryos is likely to correspond to the electron-dense matrix (EDM) (Iseto and Nishida, 1999). It is first recognizable as precursors, which appear as dozens of small dots in the posterior cortex of the 2-cell embryos. These particles gradually assemble and form a slender cluster by the 4-cell stage. During the 8-cell stage, the particles fuse together to form the CAB, which has a uniform appearance (Hibino et al., 1998; Iseto and Nishida, 1999). Injection of *POPK-1* MO also affected the distribution of CAB precursors in the 4-cell embryos. In normal embryos, the particles had already gathered to a single line (Fig. 5C,E). However, in embryos injected with *POPK-1* MO, the particles were still apart from each other and were distributed in a broader region of the posterior cortex (Fig. 5D,F). It was hard to tell whether or not the total amount of granules was less.

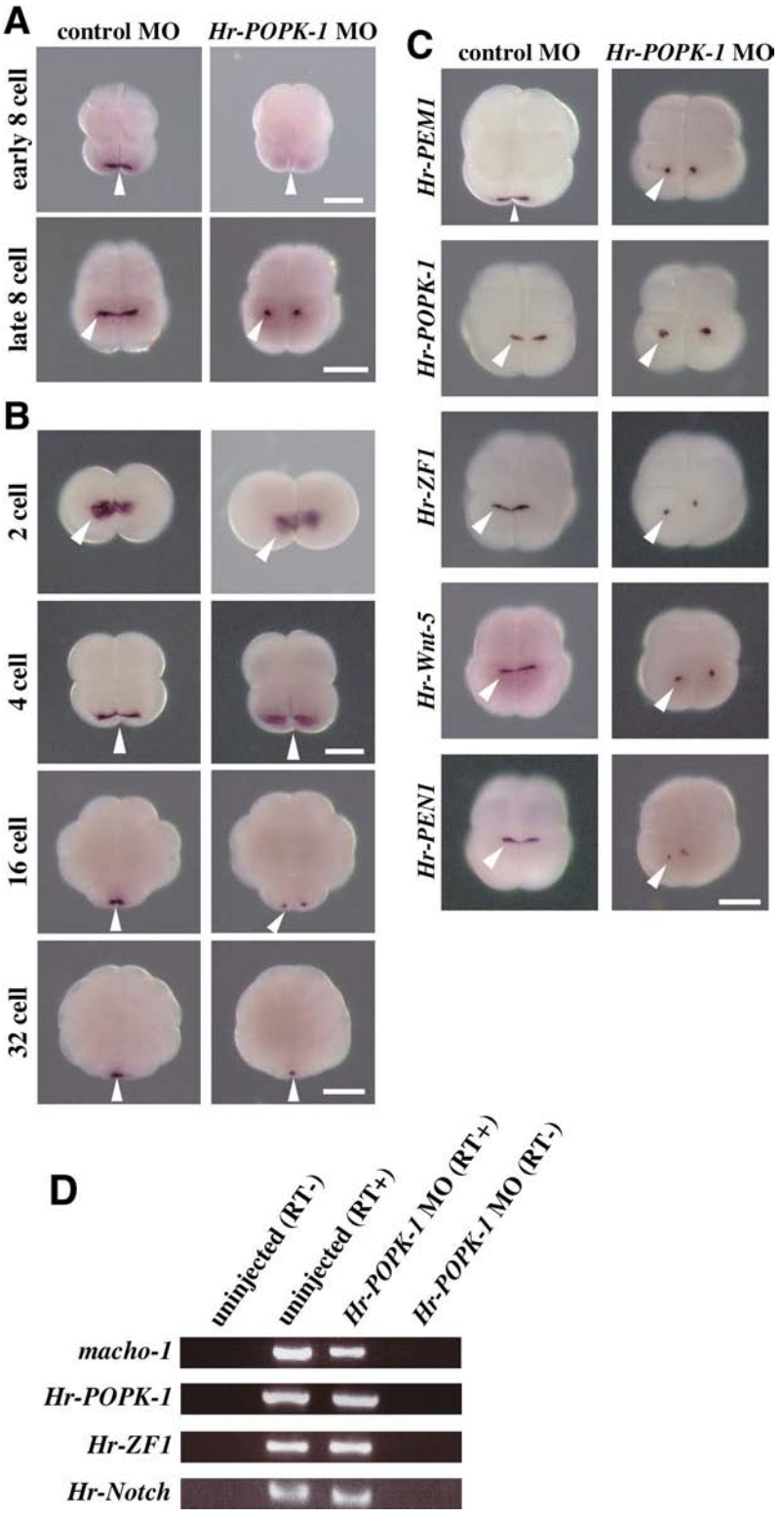

Fig. 4. Localization of *postplasmic/PEM* mRNAs in embryos injected with *Hr-POPK-1* MO. (A,B,C, left columns) Embryo injected with control MO. (A,B,C, right columns) Embryo injected with *POPK-1* MO. (A) *macho-1* localization at the early 8-cell stage (animal views), and late 8-cell stage (posterior views). (B) *macho-1* localization at the 2-cell stage (posterior views), 4-cell stage (animal views), 16-cell stage (animal views), and 32-cell stage (animal views). White arrowheads indicate *macho-1* mRNA localization. (C) Localization of various *Type I postplasmic/PEM* RNAs. The probes are indicated on the left side. Scale bars: 100 μm. (D) Semi-quantitative RT-PCR analysis of *macho-1, Hr-POPK-1*, *Hr-ZF1* and *Hr-Notch* mRNA using ten uninjected embryos (left) and ten embryos injected with *POPK-1* MO (right) at the late 8-cell stage. RT+ and RT–, with and without reverse transcriptase.

We noticed that *POPK-1* MO-injected embryos occasionally showed a radialized cleavage pattern (Fig. 6D; 34% of 112 cases), whereas all control MO-injected embryos showed unequal cleavages at the posterior pole after the 8-cell stage (Fig. 6A,B). Therefore, the correlation of the failure of unequal cleavage and shrinkage of the CAB was examined in more detail. Embryos were extracted at the 16-cell stage, and unequal cleavage and the shape of the CAB were monitored in the same embryos. Essentially, every *POPK-1* MO-injected embryo had a small CAB, but unequal cleavage still took place in most of them (Fig. 6C,E; 92% of 12 cases). However, equally cleaved embryos also had a small CAB (Fig. 6D,F). There was no difference in CAB size between the two populations.

Hr-POPK-1 regulates cER concentration into the CAB

macho-1 and *Hr-PEM1* mRNAs has been shown to associate with a cER that is tethered to the egg plasma membrane, translocate to the posterior region during ooplasmic segregation, and then concentrate into the CAB during cleavages together with the cER (Sardet et al., 2003). In the present study, we prepared isolated cortices from the unfertilized eggs and the 8-cell embryos and labeled the cER in red with the lipophilic dye $DiIC_{18}$ (3). The distribution of other *Type I postplasmic/PEM* mRNAs (*Hr-POPK-1*, *Hr-ZF1* and *Hr-Wnt-5*) was visualized with green fluorescence at high resolution using fluorescence in-situ hybridization in the same cortex. These three *Type I postplasmic/PEM* mRNAs were also co-localized with the cER network in unfertilized eggs (Fig. 7A-D), and they were highly accumulated in the CAB at the 8-cell stage (Fig. 7E-G). However, unlike *macho-1* (Fig. 7D) and *Hr-PEM1*, which are uniformly distributed on cER, the signals on entire cER were relatively weaker and, especially in *Hr-POPK-1*, some small granules with bright fluorescence were sparsely detected on tubes and sheets of the cER in unfertilized eggs (Fig. 7A-C, arrows).

Then, we examined cER distribution in *POPK-1* MO-injected embryos. As *Hr-PEM1* is the most abundant *postplasmic* RNA, we observed the distribution of *Hr-PEM1* in isolated cortices of the 8-cell embryos. In uninjected embryos, both cER and *Hr-PEM1* mRNA were concentrated in the moustache-shaped CAB, confirming the previous

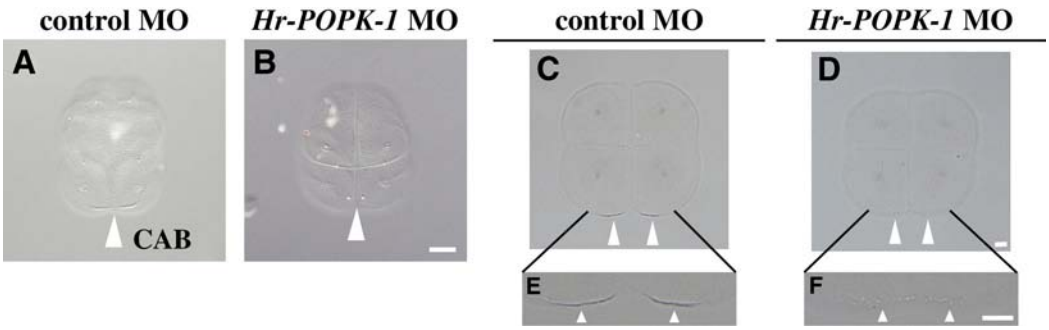

Fig. 5. CAB formation. (A,B) The CAB in extracted 8-cell embryo injected with control MO (A) and in embryo injected with *POPK-1* MO (B). Bilateral CABs are indicated by white arrowheads. Animal views. (C,D) The CAB at the 4-cell stage. (C) Control MO. (D) *POPK-1* MO. The CAB precursors are more scattered than control. (E,F) Closer views of A and C. White arrowheads indicate each CAB. Anterior is up. Scale bars: 25 μm.

observation (Fig. 8A). In embryos injected with *POPK-1* MO, the cER- and *Hr-PEM1* mRNA-rich regions were present in smaller rounded shape apart from the midline. The *Hr-PEM1* mRNA-rich region always coincided with the small cER-rich region (Fig. 8B, arrowheads). These observations indicate that POPK-1 is required for proper concentration and positioning of cER, and that it affects the mRNA distribution via cER movements.

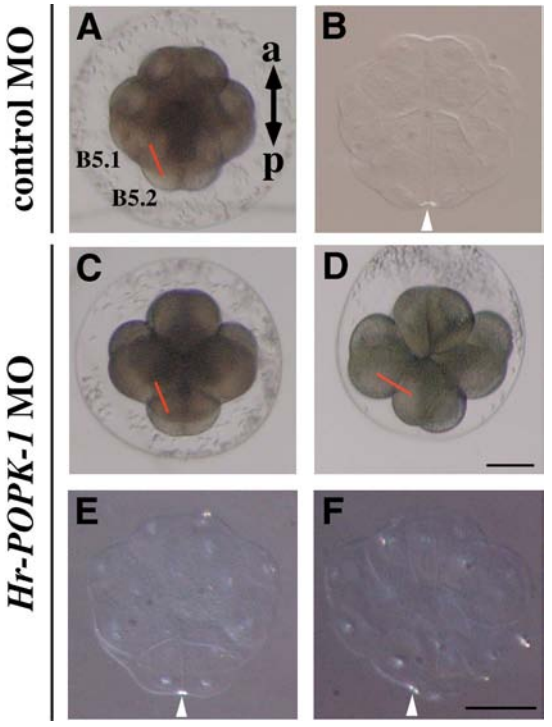

Fig. 6. Unequal cleavages in MO-injected 16-cell embryos. (A) In control embryo, B4.1 blastomeres divide into larger B5.1 and smaller B5.2 blastomeres, as indicated by red bar. (B) Normal CAB in extracted embryo. (C) In most cases, *POPK-1* MO-injected embryos also showed normal cleavage pattern. (D) Occasionally, unequal cleavage failed. (E) Unequally cleaved *POPK-1* MO-injected embryo had small CAB. (F) Even if *POPK-1* MO-injected embryos failed to divide unequally, there was always a small CAB. The shape and size of the CAB was indistinguishable from those in embryos showing unequal cleavage. Scale bar: 100 μm.

Type I postplasmic/PEM mRNA associates with the cER but not with CAB precursors at 2- and 4-cell stages

As mentioned before, in extracted embryos formation of the CAB is initiated as dozens of small dots at the 2- and 4-cell stages. However, the distribution of the *Type I postplasmic/PEM* mRNAs at the 2- and 4-cell stages did not show such a punctate and dotted appearance in whole-mount in-situ hybridization (Fig. 8C,D) (Sasakura et al., 1998a; Sasakura 1998b; Nakamura et al., 2003). In our previous study, the co-localization of *Type I postplasmic/PEM* mRNAs and the cER was observed only in eggs and 8-cell embryos (Sardet et al., 2003). Therefore, we examined the cER/mRNA distribution at the 2- and 4-cell stages in isolated cortices to investigate it in more detail. *Hr-PEM1* mRNA and cER were also clearly co-localized at these stages (Fig. 8F). However, as observed in whole mounts, a dotted distribution corresponding to the CAB precursors at these stages was never observed. Therefore, cER/mRNA distribution is not identical to that of CAB precursors in extracted embryos (probably corresponding to EDM/putative germ plasm) at these stages, although the distribution of both becomes overlapped in the CAB in the 8-cell embryos. POPK-1 is probably involved in proper concentration and positioning of both of cER/mRNA domain (Figs 4 and 8) and CAB precursors (Fig. 5) by the 8-cell stage.

Discussion

The role of *Hr-POPK-1* in localization of cER/mRNA domain

Organisms use mRNA localization to locally produce cytoplasmic factors in particular regions within cells and embryos. In ascidians, maternal *Type I postplasmic/PEM* mRNAs are localized to the PVC in fertilized eggs, and some of them have been shown to play important roles in establishment of the anteroposterior axis (Nishida and Sawada, 2001; Nakamura et al., 2005). In this study, we have presented evidence that the *postplasmic/PEM* mRNA *Hr-POPK-1* is required for the proper spatial distribution of *postplasmic/PEM*

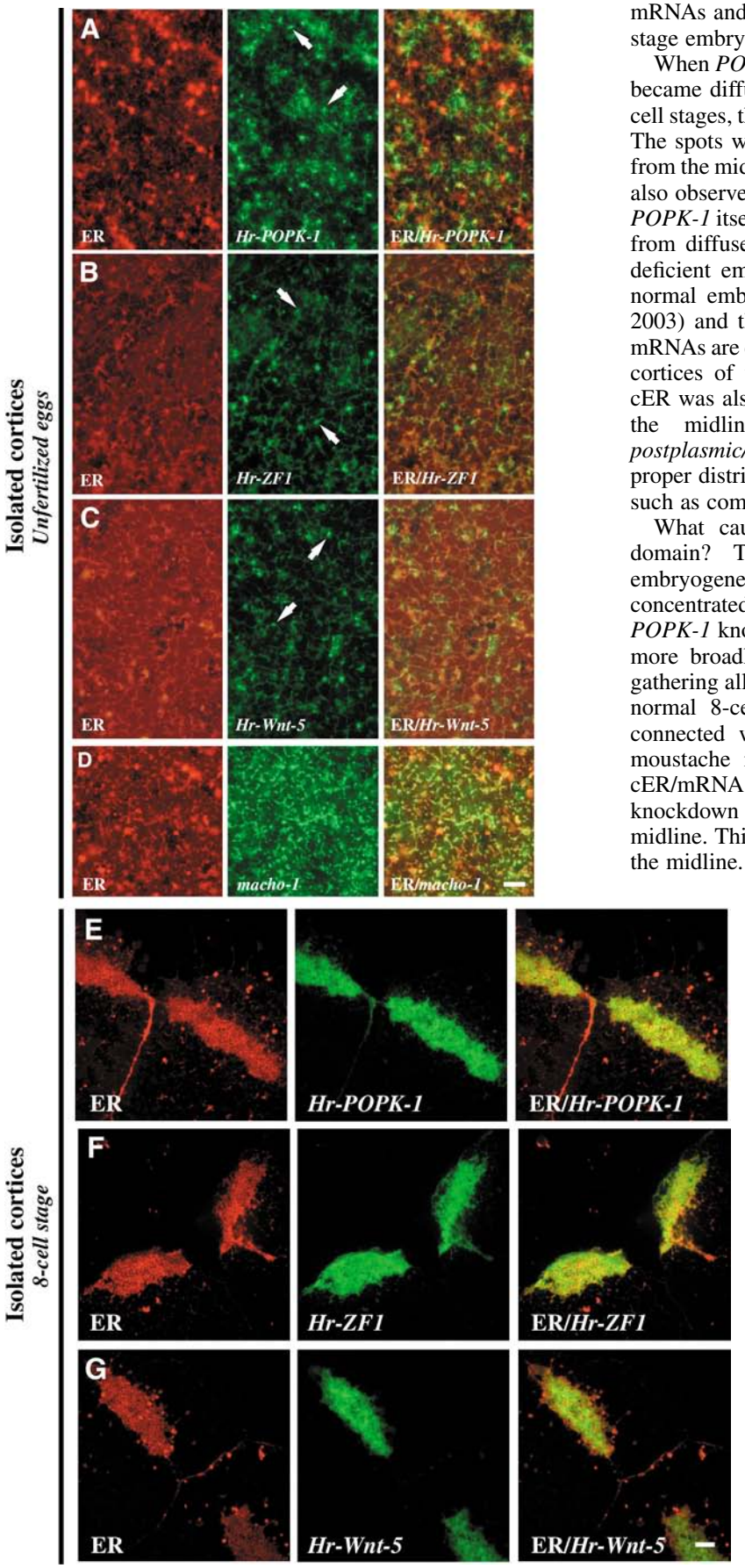

mRNAs and CAB materials at the posterior pole of cleavage-stage embryos.

When *POPK-1* MO was injected into eggs, *macho-1* mRNA became diffuse at the posterior pole at the 2-, 4 and early 8-cell stages, then detected in tiny spots after the late 8-cell stage. The spots were much smaller, rounded and always laid apart from the midline, unlike the normal moustache shape. This was also observed for all six *postplasmic/PEM* mRNAs, including *POPK-1* itself. It is not clear whether this remarkable transition from diffused to compact distribution observed in *POPK-1*-deficient embryos reflects the events that also take place in normal embryos. The results of Sardet et al. (Sardet et al., 2003) and the present data indicate that several postplasmic mRNAs are co-localized with cER and move with it. In isolated cortices of the *POPK-1* MO-injected 8-cell stage embryos, cER was also present in bilateral compact regions apart from the midline. The distribution matches that of the *postplasmic/PEM* RNA. Therefore, POPK-1 is involved in the proper distribution of mRNAs by controlling cER movements such as compaction and positioning.

What causes the reduction in size of the cER/mRNA domain? There are two possibilities. (1) In normal embryogenesis, *postplasmic/PEM* RNAs are highly concentrated into the small CAB region by the 8-cell stage. In *POPK-1* knockdown embryos, the mRNAs were spread much more broadly at the early stages. This causes difficulty in gathering all the mRNAs into the small posterior region. (2) In normal 8-cell embryos, bilateral cER/mRNA domains are connected with each other at the midline. The elongated moustache morphology implies anchoring one end of the cER/mRNA domains to the midline. But in *POPK-1* knockdown embryos, they are rounded and lie apart from the midline. This might be caused by breakup of the anchoring to the midline.

As POPK-1 has overall similarity with the proteins of a wide variety of animals, it is probably a member of a group of widely conserved proteins with shared common cellular functions among metazoans. The Sad-1 kinase of *C. elegans* is present in synapse-rich regions of axons, and mutation affects the size, shape and position of vesicle clustering in neurons (Crump

Fig. 7. *Type I postplasmic/PEM* RNA localization on isolated cortices of eggs and 8-cell embryos. cER was stained with $DiIC_{18}$ (3) and emits red fluorescence. Particle with intense red fluorescence in left panels are micelles of $DiIC_{18}$ (3). In-situ hybridization signals of *Hr-POPK-1, Hr-ZF1* and *Hr-Wnt-5* are green. (A-D) Fluorescent images of the cortices isolated from unfertilized eggs. (A) cER (left) and *Hr-POPK-1* mRNA (middle). The right panel shows a merged image. (B) cER (left), *Hr-ZF1* (middle) and a merged image (right). (C) cER (left), *Hr-Wnt-5* (middle) and a merged image (right). (D) cER (left), *macho-1* (middle) and a merged image (right). White arrowheads in A-C indicate small granules with bright green fluorescence. (E-G) Confocal images of the CAB domain in the posterior cortices isolated from 8-cell stage embryo. (E) *Hr-POPK-1* mRNA. (F) *Hr-ZF1* mRNA. (G) *Hr-Wnt-5* mRNA. Scale bars: 5 μm.

et al., 2001). Considering their common function in *C. elegans* and ascidians, these proteins may be involved in regulation of transport of intracellular organelles, especially membranous components, because POPK-1 mediates concentration and positioning of cER. The unknown conserved domains in the C-terminal half may be domains interacting with membrane-transport machinery or with cytoskeletal elements. A search in the *Drosophila* two-hybrid protein interaction database (*Drosophila* Interaction Database: http://portal.curagen.com/cgi-bin/interaction/flyHome.pl?modeIn=List) indicated with high confidence that the *Drosophila* homolog (CG6144) of POPK-1/Sad-1 interacts with CG11250. The function of CG11250 is not known, but it also encodes conserved proteins among a variety of metazoans. As POPK-1/Sad-1 is a kinase, one of the key future issues is to determine the target of phosphorylation by POPK-1/Sad-1.

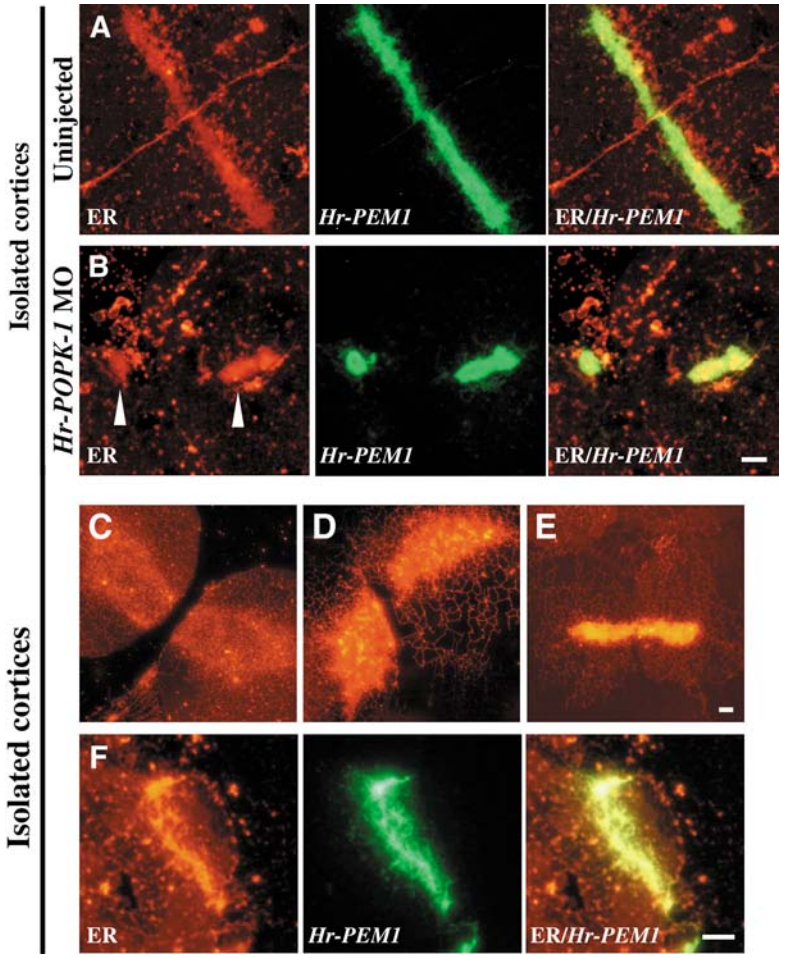

Fig. 8. Confocal images of the cER/mRNA domain in the posterior cortices in uninjected embryo and embryo injected with *POPK-1* MO. cER was stained with $DiIC_{18}$ (3) and emits red fluorescence. In-situ hybridization signal of *Hr-PEM1* is green. (A) cER (left) and *Hr-PEM1* (middle) in cortex that was isolated from an uninjected embryo at 8-cell stage. The right panel shows a merged image. (B) cER-rich domain and *Hr-PEM1*-rich domain overlap in cortices isolated from embryo injected with *POPK-1* MO. White arrowheads indicate the cER-rich region. cER/mRNA domain is smaller and rounded in embryos injected with *POPK-1* MO. (C-E) Live cortices isolated from 2-, 4-, and 8-cell embryos, respectively. (F) cER and *Hr-PEM1* mRNA in posterior cortices isolated from 4-cell stage embryo. *Hr-PEM1*-rich domain overlaps with the cER-rich domain, as shown by the merged image (right). Scale bars: 10 μm.

The role of *Hr-POPK-1* in localization of EDM/putative germ plasm

The morphology of the CAB in extracted embryos was also altered in *POPK-1* knockdown embryos. It became smaller, rounded and separate from the midline. The morphology nicely corresponded to that of the cER/mRNA domain at the 8-cell stage. The CAB precursors were more dispersed at the earlier stage compared with normal distribution (Fig. 5). One of the conspicuous characteristics of the CAB is that it is enriched in EDM, which resembles germ plasm of various kinds of animals (Iseto and Nishida, 1999). The blastomeres that inherit the CAB are thought to become primordial germ cells in ascidians (Fujimura and Takamura, 2000; Takamura et al., 2002) (reviewed by Nishida, 2005), supporting the idea that the EDM corresponds to germ plasm. In extracted embryos, only the EDM seems to persist in the CAB in electron microscopic observation (Iseto and Nishida, 1999), and it is likely that EDM is visible as a highly refractive structure under the optical microscope. Therefore, POPK-1 is also likely to be required for proper concentration and positioning of the EDM/putative germ plasm, although further analysis will be required for elucidation of the hypothesis that EDM in the CAB is equivalent to germ plasm in ascidians by detecting germ-plasm-specific molecular markers such as *Xcat2* in *Xenopus* (King et al., 2005).

At the 8-cell stage, cER/mRNA and EDM/putative germ plasm domains overlap at the posterior pole of the B4.1 blastomeres. From the 2- to 8-cell stage, the extraction-resistant CAB materials such as EDM/putative germ plasm starts to be assembled into the CAB as a number of dispersed particles, then the particles gather to form single entity (Hibino et al., 1998). By contrast, we noticed that the distribution of *postplasmic/PEM* mRNAs was broader than that of the CAB precursor particles, and not granulated (Sasakura et al., 1998a; Sasakura et al., 1998b; Nakamura et al., 2003). In the present study, we confirmed the difference in detail by using isolated cortices. The distributions of cER/mRNA and the CAB precursor particles are not precisely identical at these early stages. It appeared that concentration of cER/mRNA into the CAB and assemblage of EDM/putative germ plasm into the CAB are parallel processes, but these processes share common mechanisms that involve POPK-1. The above idea reminds us of the similar processes of maternal mRNA localization of the *Xenopus* oocyte, where two major pathways operate to localize maternal mRNAs to different but overlapping domains within the vegetal cortex during oogenesis (Heasman et al., 1984; Chang et al., 2004; King et al., 2005). One is the early pathway RNAs such as *Xcat2*, destined to become germ plasm, and another is the late pathway RNAs such as *Vg1*, which is important for animal-vegetal axis specification.

Localization of *postplasmic*/PEM mRNA into the CAB may be required for its function

In late embryogenesis, the phenotypes of embryos injected with *POPK-1* MO resembled those of the embryos injected with a low dose of *macho-1* MO. In addition, we noted that some embryos failed to undergo unequal cleavages of the posteriormost blastomeres, although no relationship was observed between the morphology of the CAB and failure of unequal division. *Hr-PEM1* is the most abundant *Type I postplasmic/PEM* mRNA in ascidian eggs (Yoshida et al., 1996; Nishida and Sawada, 2001; Makabe et al., 2001). Our recent results suggested that *Hr-PEM1* function is essential for unequal cleavage, although the morphology of the CAB after extraction was intact in *Hr-PEM1*-deficient embryos (H.N. and K. Sawada, unpublished). Therefore, the presence of CAB materials in extracted embryos is not exactly correlated with centrosome-attracting activity. Taking into account these observations, the late phenotypes of *POPK-1* knockdown embryos are probably indirect and due to partial inhibition of *macho-1* and *Hr-PEM1* functions.

Accordingly, the localization of every *postplasmic/PEM* mRNA was aberrant but not lost in *POPK-1* knockdown embryos. There could be two possibilities for how the functions of *postplasmic/PEM* mRNAs are partially inhibited. One is that mRNAs detached from the CAB-forming region might be destabilized. Loss of *POPK-1* function could cause problems in gathering all the mRNAs into the CAB at the 8-cell stage. This idea is supported by semi-quantification with RT-PCR of *macho-1* mRNA. However, the amount of *Hr-POPK-1* and *Hr-ZF1* mRNA was not altered, indicating that this hypothesis is not applicable for every *postplasmic/PEM* mRNA. Another possibility is that *postplasmic/PEM* mRNAs could not be efficiently translated outside the CAB, although we have no direct evidence to support this. However, when we injected synthetic *POPK-1* mRNA, larval development was normal. And effects of MO were not rescued by co-injection of *POPK-1* mRNA. These results may suggest that non-localized mRNA is not efficiently translated, although there are many other possibilities. Recently, it was shown that a Y-box protein (CiYB1) is involved in translational control of localized mRNAs in ascidian eggs and embryos of *Ciona* (Tanaka et al., 2004). In flies and vertebrates, the restriction of some localized mRNAs to a particular region is important for their translation in various cases (Lipshitz and Smibert, 2000; Johnstone and Lasko, 2001; Palacios and Johnston, 2001; Yoshida et al., 2004).

In *POPK-1* MO-injected embryos, localization of postplasmic mRNAs and formation of the CAB were aberrant but never completely abolished. This raises the possibility that the MOs used in this study are not able to completely inhibit the function of *POPK-1*. But this is not likely to be the case because of the following reasons. The effects of the *POPK-1* MOs were dose dependent, and the severity of the phenotype seemed saturated at the dose we used. Further, we prepared two MOs against *POPK-1*. Co-injection of the two kinds of MOs synergistically worked at low doses, and reproduced the same phenotypes. Even when we co-injected the two MOs at the original concentration, the severity of the phenotypes was not increased. Therefore, the concentrations of MOs were high enough to produce the most severe phenotype. But we could not exclude the possibility that translation of POPK-1 starts as early as the first cell cycle before we injected the MO, and already-translated POPK-1 protein exerts its residual activity.

Postplasmic/PEM mRNA localization mechanism in ascidian embryos

There are several steps by which *Type I postplasmic/PEM* mRNAs are eventually localized to the CAB. The mRNAs are located in the cortex of eggs. During ooplasmic segregation, these mRNAs are relocalized to the PVC in several cytoskeleton-driven phases (Roegiers et al., 1999; Sasakura et al., 2000). Then they concentrate into the CAB during cleavages. POPK-1 is involved in this last process.

In the present study, co-localization of the postplasmic mRNA and cER was further supported for *Hr-POPK-1*, *Hr-ZF1* and *Hr-Wnt-5*. Localization of *Type I postplasmic/PEM* mRNAs requires the presence of *cis*-elements within the 3′-UTR of mRNAs, as in other organisms (Sasakura and Makabe, 2002) (reviewed by Kloc et al., 2002). The zip code is likely to be recognized by *trans*-acting proteins that mediate attachment of the mRNAs to cER. In *Drosophila*, *gurken* is localized in oocytes and plays essential roles in defining the anterior-posterior and dorsoventral axes of the future embryo. In this system, ER is also closely associated with the mRNA (Saunders and Cohen, 1999). A mammalian homolog of Staufen, which is necessary for *bicoid* and *oskar* localization in flies, is ER-binding protein (Marion et al., 1999). In *Xenopus* oocytes, some of the maternal mRNAs co-localize with ER, and ER associates with Staufen (Allison et al., 2004; Chang et al., 2004). Therefore, co-localization of mRNA with ER would be a common phenomenon in the early development of different species. In this study, we found that *POPK-1* regulates the size and shape of the cER/mRNA domain. The results of this study will provide novel information for elucidating the localization mechanisms of maternal mRNAs in animal embryos. As POPK-1/SAD-1 is a widely conserved protein, it will be informative to examine whether the protein also works in other embryonic systems.

We thank members of the Asamushi Research Center for Marine Biology and the Otsuchi International Coastal Research Center for help in collecting live ascidian adults, and members of the Misaki Marine Biological Station and Seto Marine Biological Laboratory for help in maintaining them. We also thank Dr T. Nishikata (Konan University) for providing the Not-1 and Mu-2 monoclonal antibodies, Drs T. Kawashima (Kyoto University) and Y. Kohara (National Institute of Genetics) for the MAGEST plasmid, and Dr C. Sardet (Villefranche marine station) for critical reading of the manuscript and useful discussion. This work was supported by Grants-in-Aid for Scientific Research from JSPS and MEXT, Japan (16107005 and 13044003), and by Toray Science and Technology Grant to H.N.

References

Allison, R., Czaplinski, K., Git, A., Adegbenro, E., Stennard, F., Houliston, E. and Standart, N. (2004). Two distinct Staufen isoforms in *Xenopus* are vegetally localized during oogenesis. *RNA* **10**, 1751-1763.

Chang, P., Torres, J., Lewis, R. A., Mowry, K. L., Houliston, E. and King, M. L. (2004). Localization of RNAs to the mitochondrial cloud in *Xenopus* oocytes through entrapment and association with endoplasmic reticulum. *Mol. Biol. Cell.* **15**, 4669-4681.

Crump, J. G., Zhen, M., Jin, Y. and Bargmann, C. I. (2001). The SAD-1 kinase regulates presynaptic vesicle clustering and axon termination. *Neuron* **29**, 115-129.

Fujimura, M. and Takamura, K. (2000). Characterization of an ascidian DEAD-box gene, *CiDEAD1*: specific expression in the germ cells and its mRNA localization in the posterior-most blastomeres in early embryos. *Dev. Genes Evol.* **210**, 64-72.

Heasman, J., Quarmby, J. and Wylie, C. C. (1984). The mitochondrial cloud of *Xenopus* oocytes: the source of the germinal granule material. *Dev. Biol.* **105**, 458-469.

Hibino, T., Nishikata, T. and Nishida, H. (1998). Centrosome-attracting body: a novel structure closely related to unequal cleavages in the ascidian embryo. *Dev. Growth Diff.* **40**, 85-95.

Iseto, T. and Nishida, H. (1999). Ultrastructural studies on the centrosome-attracting body: electron-dense matrix and its role in unequal cleavages in ascidian embryos. *Dev. Growth Diff.* **41**, 601-609.

Johnstone, O. and Lasko, P. (2001). Translational regulation and RNA Localization in *Drosophila* oocytes and embryos. *Annu. Rev. Genet.* **35**, 365-406.

Karnovsky, M. J. and Roots, L. (1964). A 'direct-coloring' thiocholine method for cholinesterase. *J. Histochem. Cytochem.* **12**, 219-221.

Kim, G. J. and Nishida, H. (1998). Monoclonal antibodies against differentiating masenchyme cells in larvae of the ascidian, *Halocynthia roretzi*. *Zool. Sci.* **15**, 553-559.

King, M. L., Zhou, Y. and Bubunenko, M. (1999). Polarizing genetic information in the egg; RNA localization in the frog oocyte. *BioEssays* **21**, 546-557.

King, M. L., Messitt, T. J. and Mowry, K. L. (2005). Putting RNAs in the right place at the right time: RNA localization in the frog oocyte. *Biol. Cell* **97**, 19-33.

Kishi, M., Pan, Y. A., Crump, J. G. and Sanes, J. R. (2005). Mammalian SAD kinases are required for neuronal polarization. *Science* **307**, 929-932.

Kloc, M., Zearfoss, N. R. and Etkin, L. D. (2002). Mechanisms of subcellular mRNA localization. *Cell* **108**, 533-544.

Kobayashi, K., Sawada, K., Yamamoto, H., Wada, S., Saiga, H. and Nishida, H. (2003). Maternal *macho-1* is an intrinsic factor that makes cell response to the same FGF signal differ between mesenchyme and notochord induction in ascidian embryos. *Development* **130**, 5179-5190.

Lipshitz, H. D. and Smibert, C. A. (2000). Mechanisms of RNA localization and translational regulation. *Curr. Opin. Genet. Dev.* **10**, 476-488.

Makabe, K. W. and Satoh, N. (1989). Temporal expression of myosin heavy chain gene during ascidian embryogenesis. *Dev. Growth Diff.* **31**, 71-77.

Makabe, K. W., Kawashima, T., Kawashima, S., Minokawa, T., Adachi, A., Kawamura, H., Ishikawa, H., Yasuda, R., Yamamoto, H., Kondoh, et al. (2001). Large-scale cDNA analysis of the maternal genetic information in the egg of *Halocynthia roretzi* for a gene expression catalog of ascidian development. *Development* **128**, 2555-2567.

Marion, R. M., Fortes, P., Beloso, A., Dotti, C. and Ortin, J. (1999). A human sequence homologue of Staufen is an RNA-binding protein that is associated with polysomes and localizes to the rough endoplasmic reticulum. *Mol. Cell. Biol.* **19**, 2212-2219.

Meedel, T. H. and Whittaker, J. R. (1989). Two histospecific enzyme expression in the same cleavage-arrested one-celled ascidian embryos. *J. Exp. Zool.* **250**, 168-175.

Miya, T., Makabe, K. W. and Satoh, N. (1994). Expression of a gene for major mitochondrial protein, ADP/ATP translocase, during embryogenesis in the acidian *Halocynthia roretzi*. *Dev. Growth Diff.* **36**, 39-48.

Miya, T., Morita, K., Suzuki, A., Ueno, N. and Satoh, N. (1997). Functional analysis of an ascidian homologue of vertebrate *Bmp-2/Bmp-4* suggests its role in the inhibition of neural fate specification. *Development* **124**, 5149-5159.

Nakamura, Y., Makabe, W. K. and Nishida, H. (2003). Localization and expression pattern of type I postplasmic mRNAs in embryos of the ascidian *Halocynthia roretzi*. *Gene Expr. Patterns* **3**, 71-75.

Nakamura, Y., Makabe, W. K. and Nishida, H. (2005). The functional analysis of *Type I postplasmic/PEM* mRNAs in embryos of the ascidian *Halocynthia roretzi*. *Dev. Genes Evol.* (in press).

Nakatani, Y. and Nishida, H. (1994). Induction of notochord during ascidian embryogenesis. *Dev. Biol.* **166**, 289-299.

Nishida, H. (1994). Localization of determinants for formation of the anterior-posterior axis in eggs of the ascidian *Halocynthia roretzi*. *Development* **120**, 3093-3104.

Nishida, H. (1997). Cell fate specification by localized cytoplasmic determinants and cell interactions in ascidian embryos. *Int. Rev. Cytol.* **176**, 245-306.

Nishida, H. (2002). Specification of developmental fates in ascidian embryos: molecular approach to maternal determinants and signaling molecules. *Int. Rev. Cytol.* **217**, 227-276.

Nishida, H. (2005). Specification of embryonic axis and mosaic development in ascidians. *Dev. Dyn.* **233**, 1177-1193.

Nishida, H. and Sawada, K. (2001). macho-1 encodes a localized mRNA in ascidian eggs that specifies muscle fate during embryogenesis. *Nature* **409**, 724-729.

Nishida, H., Morokuma, J. and Nishikata, T. (1999). Maternal cytoplasmic factors for generation of unique cleavage pattern in animal embryos. *Cur. Top. Dev. Biol.* **46**, 1-37.

Nishikata, T. and Satoh, N. (1990). Specification of notochord cells in the ascidian embryo analysed with a specific monoclonal antibody. *Cell Diff. Dev.* **30**, 43-53.

Nishikata, T., Mita-Miyazawa, I., Deno, T. and Satoh, N. (1987). Muscle cell differentiation in ascidian embryos analysed with a tissue-specific monoclonal antibody. *Development* **99**, 163-171.

Nishikata, T., Hibino, T. and Nishida, H. (1999). The centrosome-attracting body, microtubule system, and posterior egg cytoplasm are involved in positioning of cleavage planes in the ascidian embryo. *Dev. Biol.* **209**, 72-85.

Palacios, I. M. and St Johnston, D. (2001). Getting the message across: the intracellular localization of mRNAs in higher eukaryotes. *Annu. Rev. Cell Dev. Biol.* **17**, 569-614.

Riechmann, V. and Ephrussi, A. (2001). Axis formation during *Drosophila* oogenesis. *Curr. Opin. Genet. Dev.* **11**, 374-383.

Roegiers, F., Djediat, C., Dumollard, R., Rouviere, C. and Sardet, C. (1999). Phases of cytoplasmic and cortical reorganizations of the ascidian zygote between fertilization and first division. *Development* **126**, 3101-3117.

Sardet, C., Nishida, H., Prodon, F. and Sawada, K. (2003). Maternal mRNAs of *PEM* and *macho 1*, the ascidian muscle determinant, associate and move with a rough endoplasmic reticulum network in the egg cortex. *Development* **130**, 5839-5849.

Sardet, C., Dru, P. and Prodon, F. (2005). Maternal determinants and mRNAs in the cortex of ascidian oocytes, zygotes and embryos. *Biol. Cell* **97**, 35-49.

Sasakura, Y. and Makabe, K. W. (2002). Identification of *cis* elements which direct the localization of maternal mRNAs to the posterior pole of ascidian embryos. *Dev. Biol.* **250**, 128-144.

Sasakura, Y., Ogasawara, M. and Makabe, K. W. (1998a). *HrWnt-5:* a maternally expressed ascidian *Wnt* gene with posterior localization in early embryos. *Int. J. Dev. Biol.* **42**, 573-579.

Sasakura, Y., Ogasawara, M. and Makabe, K. W. (1998b). Maternally localized RNA encoding a serine/threonine protein kinase in the ascidian, *Halocynthia roretzi*. *Mech. Dev.* **76**, 161-163.

Sasakura, Y., Ogasawara, M. and Makabe, K. W. (2000). Two pathways of maternal RNA localization at the posterior-vegetal cytoplasm in early ascidian embryos. *Dev. Biol.* **220**, 365-378.

Satou, Y., Imai, K. S. and Satoh, N. (2001). Action of morpholinos in *Ciona* embryos. *Genesis* **30**, 103-106.

Saunders, C. and Cohen, R. S. (1999). The role of oocyte transcription, the 5′UTR, and translation repression and derepression in *Drosophila gurken* mRNA and protein localization. *Mol. Cell* **3**, 43-54.

Takamura, K., Fujimura, M. and Yamaguchi, Y. (2002). Primordial germ cells originate form the endodermal strand cells in the ascidian *Ciona intestinalis*. *Dev. Genes Evol.* **212**, 11-18.

Tanaka, K. J., Matsumoto, K., Tsujimoto, M. and Nishikata, T. (2004). CiYB1 is a major component of storage mRNPs in ascidian oocytes: implications in translational regulation of localized mRNAs. *Dev. Biol.* **272**, 217-230.

Whittaker, J. R. (1973). Segregation during ascidian embryogenesis of egg cytoplasmic information for tissue-specific enzyme development. *Proc. Natl. Acad. Sci. USA* **70**, 2096-2100.

Yoshida, S., Marikawa, Y. and Satoh, N. (1996). *posterior end mark*, a novel maternal gene encoding a localized factor in the ascidian embryo. *Development* **122**, 2005-2012.

Yoshida, S., Muller, H. J., Wodarz, A. and Ephrussi, A. (2004). PKA-R1 spatially restricts Oskar expression for *Drosophila* embryonic patterning. *Development* **131**, 1401-1410.